Clim. Past Discuss., 11, 1177–1218, 2015
www.clim-past-discuss.net/11/1177/2015/
doi:10.5194/cpd-11-1177-2015

Climate of the Past
Discussions
Open Access

Short-term variability in the sedimentary BIT index of Lake Challa, East Africa over the past 2200 years: validating the precipitation proxy

L. K. Buckles[1], J. W. H. Weijers[1,*], D. Verschuren[2], C. Cocquyt[2,3], and J. S. Sinninghe Damsté[1,4]

[1]University of Utrecht, Faculty of Geosciences, P.O. Box 80.021, 3508 TA Utrecht, the Netherlands
[2]Limnology Unit, Department of Biology, Ghent University, K. L. Ledeganckstraat 35, 9000 Gent, Belgium
[3]Botanic Garden Meise, Nieuwelaan 38, 1860 Meise, Belgium
[4]NIOZ Royal Netherlands Institute for Sea Research, Department of Marine Organic Biogeochemistry, P.O. Box 59, 1790 AB Den Burg, Texel, the Netherlands
[*]now at: Shell Global Solutions International B. V., Kessler Park 1, 2288 GS Rijswijk, the Netherlands

Received: 9 February 2015 – Accepted: 3 March 2015 – Published: 2 April 2015

Correspondence to: J. S. Sinninghe Damsté (jaap.damste@nioz.nl)

Published by Copernicus Publications on behalf of the European Geosciences Union.

Abstract

The branched vs. isoprenoid index of tetraethers (BIT index) in Lake Challa sediments has been applied as a monsoon precipitation proxy on the assumption that the primary source of branched tetraether lipids (brGDGTs) was soil washed in from the lake's catchment. However, water column production has since been identified as the primary source of brGDGTs in Lake Challa, meaning that there is no longer a clear mechanism linking BIT index variation and precipitation. Here we investigate BIT index variation and GDGT concentrations at a decadal resolution over the past 2200 years, in combination with GDGT data from profundal surface sediments and 45 months of sediment-trap deployment.

The 2200 year record reveals high-frequency variability in GDGT concentrations, and therefore the BIT index. Also surface sediments collected in January 2010 show a distinct shift in GDGT composition relative to those collected in August 2007. Increased bulk flux of settling particles with high Ti / Al ratios during March–April 2008 reflect an event of high detrital input to Lake Challa, concurrent with intense precipitation at the onset of the principal rain season that year. Although brGDGT distributions in the settling material are initially unaffected, this soil erosion event is succeeded by a large diatom bloom in July–August 2008 and a concurrent increase in GDGT-0 fluxes. Near-zero crenarchaeol fluxes indicate that no thaumarchaeotal bloom developed during the subsequent austral summer season; instead a peak in brGDGT fluxes is observed in December 2008. We suggest that increased nutrient availability, derived from eroded soil washed into the lake, stimulated both diatom productivity and the GDGT-0 producing archaea which help decompose dead diatoms passing through the suboxic zone of the water column. This disadvantaged the Thaumarchaeota that normally prosper during the following austral summer. Instead, a bloom of supposedly heterotrophic brGDGT-producing bacteria occurred.

Episodic recurrence of such high soil-erosion events, integrated over multi-decadal and longer timescales and possibly enhanced by other mechanisms generating low

BIT index values in dry years, can explain the positive relationship between the sedimentary BIT index and monsoon precipitation at Lake Challa. However, application elsewhere requires ascertaining the local situation of lacustrine brGDGT production and of variables affecting the productivity of Thaumarchaeota.

1 Introduction

Geographically widespread isoprenoid and branched glycerol dialkyl glycerol tetraether (iso/brGDGT) membrane lipids have allowed the development of several new molecular proxies used in palaeoenvironmental reconstruction (e.g. Schouten et al., 2002, 2013; Hopmans et al., 2004; Weijers et al., 2007a). Although isoGDGTs can be found in soil (Leininger et al., 2006) and peat (Weijers et al., 2004, 2006), they are generally most abundant in marine and freshwater environments (Sinninghe Damsté et al., 2002; Blaga et al., 2009). IsoGDGT-producing Thaumarchaeota (Brochier-Armanet et al., 2008; Spang et al., 2010; earlier referred to as Crenarchaeota, e.g. Wuchter et al., 2006) are now known to occur in most medium to large lakes (Blaga et al., 2009). Since brGDGTs were originally thought to be produced solely in soil and peat (e.g. Hopmans et al., 2004; Weijers et al., 2007a; Schouten et al., 2013), the Branched vs. Isoprenoid Tetraether (BIT) index was developed as a proxy for soil organic matter input in marine sediments (Hopmans et al., 2004; Weijers et al., 2009). BIT expresses the abundance of brGDGTs relative to crenarchaeol, the characteristic membrane lipid of pelagic Thaumarchaeota (Sinninghe Damsté et al., 2002; Pitcher et al., 2011). Subsequently, the BIT index was extended to lake sediments (e.g. Verschuren et al., 2009; Wang et al., 2013). However, this application has become complicated by recent indications of brGDGT production within lakes (e.g., Tierney and Russell, 2009; Tierney et al., 2010; Loomis et al., 2011). Also in Lake Challa, in situ production has been identified in the water column (Sinninghe Damsté et al., 2009; Buckles et al., 2014a) and suggested, but not confirmed, in profundal surface sediments (Buckles et al., 2014a).

Rainfall variability in equatorial East Africa is governed by biannual passage of the Intertropical Convergence Zone (ITCZ), with the intensity of northeasterly and southeasterly monsoons strongly linked to precessional insolation forcing at long time scales (Verschuren et al., 2009), and to El Niño Southern Oscillation (ENSO) dynamics at inter-annual time scales (Wolff et al., 2011). Verschuren et al. (2009) presented a 25 000 year BIT index record for Lake Challa near Mt. Kilimanjaro, which corresponded well with both known climatic events for the region and the succession of local lake highstands and lowstands evidenced in high-resolution seismic-reflection data. The BIT index was thus interpreted to reflect changes in the amount of soil-derived brGDGTs, associated with variation in the rate of soil erosion that was assumed proportional to rainfall intensity. The recent evidence for overwhelming in situ production of brGDGTs within Lake Challa (Buckles et al., 2014a) implies that the BIT index may not respond (or at least not directly) to a variable influx of soil organic matter, but is rather controlled by the in-lake production of crenarchaeol by Thaumarchaeota (Sinninghe Damsté et al., 2012a). Strong dependence of the BIT index in Lake Challa sediments on crenarchaeol abundance, rather than brGDGT abundance, was also evident in an almost 3 year monthly time series of settling particles (Buckles et al., 2014a). The precise mechanism(s) by which the BIT index responds to changes in precipitation has thus remained elusive. Further investigating the issue, we here present a 2200 year record of GDGT distributions in the Lake Challa sediment record with decadal resolution, with the aim to bridge the resolution (and thus information) gap between our time series of sediment-trap data and the 25 000 year climate-proxy record. To this end, we also analyse GDGT distributions in a chronosequence of recent profundal surface sediments.

CPD
11, 1177–1218, 2015

2 Materials and methods

2.1 Study site

Lake Challa is a 4.2 km^2 crater lake in equatorial East Africa, situated at 880 m elevation in the foothills of Mt. Kilimanjaro. High crater walls (up to 170 m) confine a small catchment area of 1.38 km^2, which during periods of exceptional precipitation can enlarge to 1.43 km^2 due to activation of a small creek in the NW corner of the lake (Fig. 1). The water budget of this deep lake (92 m in 2005) is dominated by groundwater, which accounts for ca. 80 % of hydrological inputs and is mostly derived from rainfall on the montane forest zone of Mt. Kilimanjaro (1800 to 2800 m elevation; Hemp, 2006). Passage of the Intertropical Convergence Zone (ITCZ) twice annually results in a short and a long rainy season. "Long rains" occur from March to mid-May, while typically more intense "short rains" stretch from late October to December (e.g. Verschuren et al., 2009; Wolff et al., 2011). Over the course of sediment-trap deployment, a long drought stretched from May 2007 to February 2008 due to failure of the short rains in 2007 (Fig. 2a). Air temperatures at the lake are lowest (20–21 °C; 24 h average) in July–August (austral winter), and the highest (∼ 25 °C; 24 h average) in January–February (austral summer; data provided by A. Hemp, University of Bayreuth; cf. Buckles et al., 2014a). The lake surface water is coolest (∼ 23 °C) between June and September, promoting seasonal deep mixing that reaches down to 40–60 m depth. During austral summer from February to April, the surface water is ∼ 28 °C, and experiences daily stratification followed by wind-driven and convective mixing down to 15–20 m depth (Wolff et al., 2014). The bottom water of Lake Challa is constantly 22.3 °C and permanently anoxic, since it does not mix even on a decadal scale. The finely laminated profundal sediments of Lake Challa (Wolff et al., 2011) contain diatom silica mainly deposited during the months of deep seasonal mixing (Barker et al., 2011), alternating with organic matter and calcite laminae that are deposited during the austral spring and summer to produce alternating dark/light layers.

CPD
11, 1177–1218, 2015

2.2 Sampling

The composite sediment sequence studied here mostly consists of a mini-Kullenberg piston core (CH03-2K; 2.6 m) recovered in 2003 from a mid-lake location (Fig. 1), supplemented at the top by a cross-correlated gravity core (CH05-1G) and a short section of a Uwitec hammer-driven piston core (CH05-3P-I) recovered in 2005 (Verschuren et al., 2009; Wolff et al., 2011). The detailed age model available for this core is a smoothed spline through INTCAL04 calibrated AMS ^{14}C ages of bulk organic carbon, corrected for an evolving old-carbon age offset (Blaauw et al., 2011). The sequence studied here covers the period between ca. 2150 cal yr BP (ca. 200 BCE) and the present. It is also covered by a varve-based chronology (Wolff et al., 2011) fully consistent with the ^{14}C chronology, demonstrating continuity of deep-water sediment deposition throughout this period. In this study, we examined 208 integrated 1 cm-sediment intervals from 0 to 213 cm depth, sampled contiguously with the exception of five intervals (23–24, 28–29, 99–100, 100–101 and 153–154 cm) where previous analyses had depleted the available material. Each interval of the time series thus represents 10.4 years, on average. Percentage of organic carbon (% C_{org}) data are based on determination of the percentage of organic matter (% OM) at contiguous 1 cm intervals, obtained by the loss-on-ignition (LOI) method (Dean, 1974) and using a linear regression against coupled % C_{org} values obtained on a subset of the same intervals. These % C_{org} values were determined through combustion of acidified sediment samples on a Fisons NA1500 NCS elemental analyser (EA) using the Dumas method (courtesy of Birgit Plessen, GFZ-Potsdam).

2.3 Diatom analysis

A preserved subsample of the filtered sediment-trap material (1/8 of the filter) was used for diatom analyses. Diatom valves present on the filter were brought back in suspension with distilled water; afterwards, filters were carefully checked for any remaining material. The obtained suspension was then diluted to a known volume and quantita-

CPD
11, 1177–1218, 2015

tively studied following the Uthermöhl (1931) method using sedimentation chambers of 10 mL and an inverted Olympus CX41 microscope, working with an oil immersion objective of 100 times.

2.4 GDGT analysis

Freeze-dried sediments (1–2 g) were extracted with a dichloromethane (DCM) / methanol solvent mixture (9 : 1, v/v) using a Dionex accelerated solvent extraction (ASE) instrument at high temperature (100 °C) and pressure (1000 psi). Each extract was rotary evaporated to near-dryness and separated by column chromatography using Al_2O_3 stationary phase, with the first (apolar) fraction eluted by hexane : DCM (9 : 1, v : v) and the second (polar) fraction by DCM: methanol (1 : 1, v : v). 0.1 µg of C_{46} GDGT standard (cf. Huguet et al., 2006) was added to the polar fraction. The apolar fraction was archived.

Analysis of the sediment-trap material and recently deposited surface sediments has been described elsewhere (Buckles et al., 2014a). Here we report additional results for GDGTs I to IV (see Appendix for structures) present in these samples. Sinking particulate matter was sampled at a central location on a near-monthly basis from 18 November 2007 to 31 August 2010, and surface sediments were sampled at seven mid-lake locations in January 2010 (Fig. 1). These samples were processed for GDGT analysis in a slightly different way than core samples (Buckles et al., 2014a). In short, sediment-trap material as well as surface sediments were extracted using a modified Bligh–Dyer method, yielding both intact polar lipid (IPL) and core lipid (CL) GDGTs. IPL GDGTs were separated from CL GDGTs using column chromatography with an activated silica gel stationary phase, using hexane : ethyl acetate 1 : 1 (v/v) and methanol to elute CL and IPL GDGTs, respectively. IPL GDGTs were subsequently subjected to acid hydrolysis to remove the functional head groups and analysed as CL GDGTs.

Each fraction was dissolved in hexane : isopropanol 99 : 1 (v : v) and passed through PTFE 0.45 µm filters prior to high-performance liquid chromatography/atmospheric pressure chemical ionisation – mass spectrometry (HPLC/APCI-MS). This used an Ag-

CPD
11, 1177–1218, 2015

ilent 1100 series HPLC connected to a Hewlett-Packard 1100 MSD SL mass spectrometer in selected ion monitoring (SIM) mode, using the method described by Schouten et al. (2007). A standard mixture of crenarchaeol : C_{46} GDGT was used to check, and to account for, differences in ionisation efficiencies.

GDGT distributions in the samples were quantified using the following indices:

$$\text{BIT index} = \frac{[\text{VI}] + [\text{VII}] + [\text{VIII}]}{[\text{VI}] + [\text{VII}] + [\text{VIII}] + [\text{V}]} \tag{1}$$

$$\text{MBT} = \frac{[\text{VI}] + [\text{VIb}] + [\text{VIc}]}{[\text{VI}] + [\text{VIb}] + [\text{VIc}] + [\text{VII}] + [\text{VIIb}] + [\text{VIIc}] + [\text{VIII}] + [\text{VIIIb}] + [\text{VIIIc}]} \tag{2}$$

$$\text{DC} = \frac{[\text{VIb}] + [\text{VIIb}]}{[\text{VI}] + [\text{VIb}] + [\text{VII}] + [\text{VIIb}]} \tag{3}$$

The fractional abundance of each individual GDGT is expressed as:

$$f[\text{GDGT}i] = \frac{[\text{GDGT}i]}{[\Sigma\,\text{GDGTs}]} \tag{4}$$

where $f[\text{GDGT}i]$ = fractional abundance of an individual GDGT, $[\text{GDGT}i]$ = concentration of the individual GDGT, based on surface area relative to the C_{46} standard, and $[\Sigma\text{GDGTs}]$ = the summed concentration of all measured GDGTs (I to VIIIc, see Appendix).

The proportion of IPL compared to CL GDGTs is expressed using % IPL, defined as:

$$\%\text{IPL} = \left(\frac{[\text{IPL}]}{[\text{IPL}] + [\text{CL}]}\right) \times 100 \tag{5}$$

where [IPL] = intact polar lipid concentration and [CL] = core lipid concentration. IPLs represent living, GDGT-producing bacteria/archaea (e.g. Lipp and Hinrichs, 2009; Pitcher et al., 2011b; Schubotz et al., 2009; Lengger et al., 2012; Schouten et al., 2012; Gibson et al., 2013).

CPD
11, 1177–1218, 2015

Short-term variability in the sedimentary BIT index of Lake Challa

L. K. Buckles et al.

2.5 Statistical analysis

Pearson product-moment correlation coefficients were calculated on un-smoothed time-series data of the core sequence, using a two-tailed test of significance in IBM SPSS Statistics 21, with bootstrapping at the 95 % confidence interval and missing values excluded pairwise. Linear varve thicknesses (Wolff et al., 2011) were averaged over the depth intervals of GDGT analysis. Following general guidelines, the strength of (positive/negative) correlation was considered weak if less than 0.3, moderate from 0.3 to 0.5, and strong from upwards of 0.5.

3 Results

3.1 The 2200 year BIT-index record

The percentage total organic carbon (% C_{org}) in the composite sediment sequence (Table S1 in the Supplement) varies from 4.4 to 12.5 %, with the lowest values generally grouping between 1200 and 1830 AD (Fig. 3a). The concentrations of GDGTs quoted here are expressed relative to C_{org} content, unless otherwise stated. The concentration of GDGT-0 (GDGT-I; Appendix) varies widely (97 to 921 $\mu g\,g^{-1}$ C_{org} and SD of 150 $\mu g\,g^{-1}$ C_{org}; Table S1) and at an average of 273 $\mu g\,g^{-1}$ C_{org} is generally high. A baseline concentration of 200–400 $\mu g\,g^{-1}$ C_{org} is interrupted by relatively long-term pulses of > 500 $\mu g\,g^{-1}$ C_{org} (Fig. 3b), the longest of which stretch from around AD 100 to 200, AD 300 to 500 and AD 1200 to 1400.

Crenarchaeol fluctuates by two orders of magnitude between 9 and 412 $\mu g\,g^{-1}$ C_{org} (ca. 1210 and 1810 AD respectively; SD of 64 $\mu g\,g^{-1}$ C_{org} Table S1). Periods of high crenarchaeol (> 150 $\mu g\,g^{-1}$ C_{org}) occur from around AD 400 to 450, AD 1250 to 1300 and AD 1700 to 1850 (Fig. 3c). The proportion of the crenarchaeol regioisomer with respect to crenarchaeol (GDGT $V'/(V+V')$) is relatively low and constant at around

CPD
11, 1177–1218, 2015

2.5 to 3 % throughout the analysed core sequence (with a maximum of 4.0 % around 730 AD; Fig. 3d), confirming that the majority of recovered crenarchaeol originates from aquatic, rather than soil, Thaumarchaeota (cf. Sinninghe Damsté et al., 2012a, b).

The concentration of total brGDGTs relative to % C_{org} varies by one order of magnitude between 94 and 493 $\mu g\,g^{-1}$ C_{org} (Table S1). BrGDGT concentrations are higher, on average, than those of crenarchaeol (197 vs. 113 $\mu g\,g^{-1}$ C_{org}, respectively; brGDGT SD of 68 $\mu g\,g^{-1}$ C_{org}) but similarly display a baseline (here between 200 and 250 $\mu g\,g^{-1}$ C_{org}; Fig. 3e) interspersed by peaks of which the timing generally corresponds with those reported for crenarchaeol. This trend persists when using absolute concentrations in $\mu g\,g^{-1}$ dry weight). In fact, brGDGT concentrations correlate strongly with crenarchaeol concentrations and those of its regioisomer ($r = 0.67$ and 0.67; Table S2).

The BIT index ranges between 0.42 (101–102 cm; ca. AD 1175) and 0.93 (142–143 cm; ca. AD 730), with an average of 0.65 ± 0.09 (Table S1). Generally higher BIT values are evident from ca. AD 650 to 950 (Fig. 3f), followed first by a period of lower BIT values (ca. AD 1150 to 1270) and then a period of higher BIT values (ca. AD 1550 to 1700). Following a 60 yr period of lower BIT values (AD 1770 to 1830), an overall increase to the present is interrupted by two ~ 30 yr periods of lower BIT values, in the late 19th century and the mid-20th century. The BIT index does not correlate with the concentrations of any brGDGTs, but shows strong negative correlation with the concentrations of crenarchaeol and its regioisomer ($r = -0.70$ and -0.68, respectively; Table S2). The BIT index also correlates with measures of brGDGT distribution: moderately positive with MBT ($r = 0.44$) but weakly so with DC ($r = 0.16$; Table S2). MBT values (ranging 0.40 to 0.54) and DC (0.15 to 0.26) themselves do not vary widely (Fig. 4; Table S1).

CPD
11, 1177–1218, 2015

3.2 Settling particles

Results for bulk sediment flux, % C_{org}, crenarchaeol and brGDGTs in the monthly sediment-trap time series have been presented elsewhere (Sinninghe Damsté et al., 2009; Buckles et al., 2014a). Here they are shown (Fig. 2b, d and e) as reference for new data on the CL and IPL fractions of GDGT-0 (Fig. 2c). Fluxes of IPL GDGT-0 in settling particles are generally low (0.3–0.4 $\mu g\,m^{-2}\,day^{-1}$) from the start of its measurement in December 2007 until June 2008 (Fig. 2c, Table S3), but subsequently peak at 7.7 $\mu g\,m^{-2}\,day^{-1}$ in August 2008 at the height of a massive, mixing-season diatom bloom (Fig. 2b) After this maximum, IPL GDGT-0 fluxes vary between 0.0 and 1.7 $\mu g\,m^{-2}\,day^{-1}$, with an additional peak of 2.8 $\mu g\,m^{-2}\,day^{-1}$ in September 2009, again coincident with a (now smaller) seasonal diatom bloom (Barker et al., 2011). CL GDGT-0 fluxes track those of IPL GDGT-0 but are notably lower, ranging from < 0.05 to 2.0 $\mu g\,m^{-2}\,day^{-1}$ (Table S3). From December 2007 to the end of August 2008, IPL GDGT-0 contribute a flux-weighted average of 77 % to total GDGT-0.

3.3 Surface sediments

Sinninghe Damsté et al. (2009) and Buckles et al. (2014a) presented data on % C_{org}, crenarchaeol (including its regioisomer), GDGT-0 and brGDGTs in Lake Challa surface sediments collected in, respectively, August 2007 (from gravity core CH07-1G: 0–0.5 and 0.5–1 cm depth, here combined into a single result for 0–1 cm) and January 2010 (seven CH10 gravity core tops, all 0–1 cm depth). Here they are shown again (Figs. 5b, c and 6a, c) as reference for new data on the 2200 yr sediment record and on IPL and CL GDGT-0 (Tables 1 and S4). IPL and CL GDGT-0 concentrations in CH10 surface sediments are, on average, 14.5 and 8.7 $\mu g\,g^{-1}$ dry wt. (Table 1). The dominant GDGT in these sediments is GDGT-0, with fractions of 0.85 (IPL) and 0.49 (CL) (Fig. 6a; Table 1). Additionally, IPL GDGT-0 represents on average 61 % of total GDGT-0.

4 Discussion

4.1 Temporal variability in sedimentary GDGT composition and BIT index

The 2200 year, decadal-resolution organic geochemical record of Lake Challa shows a great deal of variation in GDGT composition (Fig. 3b–e), particularly with respect to the concentrations of brGDGTs and crenarchaeol that underpin the BIT index. Here we quantified the absolute GDGT concentrations, which had not been examined for the 25 000 yr, lower-resolution record (Verschuren et al., 2009; Sinninghe Damsté et al., 2012a), allowing greater insight into the factors potentially affecting the BIT index over time. Our 2200 year record is generated from the upper portion of the same composite core sequence, consequently it generates comparable BIT values (both in absolute values and variability) when averaged over four adjacent 1 cm samples to mimic the measurements on homogenized 4 cm increments of the low-resolution record (Fig. 3g). This demonstrates that the lower-resolution analysis fails to capture strong variation in sedimentary GDGT concentrations (and therefore in the BIT index) on short timescales (Fig. 3b–e). To better understand this high-frequency variability, we first evaluate what can be learned from variability in the present-day system as reflected in the sediment-trap time series and in our chronosequence of surface sediments.

4.2 GDGT variability in Lake Challa settling particles and surface sediments

The soft, uncompacted top centimetre of mid-lake profundal surface sediments in Lake Challa represents approximately two years of deposition (Sinninghe Damsté et al., 2009; see also Blaauw et al., 2011). CH07 can, therefore, be treated as broadly representing the period from mid-2005 to August 2007, and CH10 the period from early 2008 to January 2010. By comparison, one centimetre of compacted sediments in our 2200 year record represents about a decade of deposition.

GDGTs in the CH10 surface sediments are dominated by GDGT-0 and brGDGTs, with relatively low proportions of crenarchaeol (Fig. 5a–c). IPL and CL BIT index values are therefore high at ca. 0.90 (Table 1; Fig. 5d). This differs markedly from the CL GDGT composition of CH07 surface sediment (Sinninghe Damsté et al., 2009). CH07 has a higher proportion of crenarchaeol than either brGDGTs or GDGT-0 (Fig. 5a–c), and consequently a lower BIT index value (0.50; Fig. 5d). This shift in fractional abundances is also reflected in the absolute concentrations (Table 1). The BIT index difference between CH10 and CH07 surface sediments is consistent with BIT index trends in settling particles, which are higher, on average, over the period covered by CH10 (Fig. 2f, highlighted in blue) than over the period covered by CH07 (Fig. 2f, highlighted in green). Whereas 45 months of sediment trapping has yielded BIT index values ranging between 0.09 and 1.00, the absolute difference (0.40) between BIT index values of the temporally more integrated surface sediment samples CH07 and CH10 is comparable to the full range of BIT index variation in the 2200 year sediment record (Fig. 5d). Our monthly collections of settling particles also yield far greater differences in GDGT distribution (Fig. 2c–f) and brGDGT composition (Fig. 4) than any other sample group. This implies that a still higher-resolution geochemical analysis of a long sediment record would yield even greater temporal variation in GDGT distribution than observed in this study, at least in the case of Lake Challa where seasonal variation in the composition of settling materials is preserved intact as finely laminated sediments with annual rhythm (Wolff et al., 2014).

Since the brGDGTs and crenarchaeol found in Lake Challa sediments are thought to be primarily produced between 20 and 40 m depth (Buckles et al., 2013, 2014a), it is tempting to attribute these rapid changes in the GDGT composition of descending particles and surface sediments to shifts in the GDGT-producing community within the water column. In Lake Challa, crenarchaeol is produced by Thaumarchaeota that have bloomed annually during the austral summer (between November and February) in three out of four monitored years (Fig. 2e). Its production in the suboxic zone between 20 and 45 m depth (Buckles et al., 2013) is where the majority of GDGTs found in surface sediments originate (Buckles et al., 2014a). Thus, data from settling particles trapped at 35 m depth can be used to assess the amounts and distribution of

CPD
11, 1177–1218, 2015

Short-term variability in the sedimentary BIT index of Lake Challa

L. K. Buckles et al.

GDGTs exported to the sediments. Here, we examine fluxes of settling particles (Sinninghe Damsté et al., 2009; Buckles et al., 2014a) integrated over the time period from November 2006 to August 2007 and from February 2008 to January 2010 (Table 2). Encompassing the two years prior to collection of our CH10 surface-sediment samples, the latter period is taken to represent the contribution of GDGTs from the water column to CH10 sediments (0–1 cm depth). The former period encompasses just under a year of deposition prior to collection of CH07 surface sediments and thus does not cover the two years of deposition approximately represented by its 0–1 cm interval, however GDGT compositions of the 0–0.5 and 0.5–1.0 cm intervals (analysed separately; Table S4) are comparable.

Comparison of these two types of time-integrated samples (Fig. 6a–d) shows, simultaneously, the strong contrast in the distribution of GDGTs exported to Lake Challa sediments during these two time periods (cf. Fig. 5a–d), and the good overall correspondence between GDGT distributions in settling particles and surface sediments that represent the same period (Fig. 6a, b vs. c, d). CL GDGT-0 is present in higher proportions in CH10 and CH07 surface sediments than in settling particles (Fig. 6a, c vs. b, d), likely indicating additional production within the bottom sediments and/or in the water column below 35 m depth (cf. Buckles et al., 2014a). BrGDGTs (GDGTs VI–VIII) appear to have similar proportions in sediments and settling particles (accounting for the difference in GDGT-0). However, MBT indices of the two sample groups are slightly offset (Fig. 4). This is also most likely due to a (small) contribution by sedimentary brGDGT production, as identified previously by Buckles et al. (2014a). Besides these minor differences, the GDGT distributions in settling particles during both periods largely replicate the contrast in GDGT distribution between CH10 and CH07. As the former are due to changes in the GDGT-producing community within the upper part of the water column, we can use our monthly GDGT-flux time series to determine the cause(s) of short-term shifts in sedimentary GDGT distribution.

CL crenarchaeol fluxes in settling particles reached three clear peaks, indicating thaumarchaeotal blooms, in January 2007 (9 µg m^{-2} day^{-1}, Fig. 2e; Table S3), Decem-

CPD
11, 1177–1218, 2015

ber 2007 to January 2008 (3 µg m^{-2} day^{-1}) and March to April 2010 (4 µg m^{-2} day^{-1}). IPL crenarchaeol fluxes (where available) were an order of magnitude lower than, but co-varied with CL fluxes. IPL GDGT-1, -2 and -3 fluxes co-varied with crenarchaeol (Table S3), indicating that they are primarily produced by Thaumarchaeota (previously discussed by Buckles et al., 2014a). In contrast, CL brGDGT fluxes peaked at 12 µg m^{-2} day^{-1} between mid-November and December 2006 (Fig. 2d) and at 10 µg m^{-2} day^{-1} in December 2008. Concurrent with maxima in IPL brGDGTs, they are likely due to blooms of brGDGT-producing bacteria in the water column (Buckles et al., 2014a). Although both maxima occurred near the end of the short rain season and may thus represent a seasonal bloom, they occurred in only two of four such seasons that we monitored. Since the first peak in brGDGT fluxes occurred during deposition of CH07 and the second during deposition of CH10, this may account for their similar brGDGT concentrations (Table 1; Figs. 5c and 6a–c).

GDGT-0 fluxes were high (CL: ca. 1 µg m^{-2} day^{-1}; IPL not measured) between mid-November and December 2006 but declined to near-zero values by March 2007 (Fig. 2c; Table S3). GDGT-0 fluxes peaked again in August 2008 (2 and 8 µg m^{-2} day^{-1}, respectively, for CL and IPL). During these maxima, crenarchaeol and cyclic isoGDGTs did not co-vary with GDGT-0, confirming a separate source for GDGT-0 in the water column as previously suggested (Sinninghe Damsté et al., 2009, 2012a; Buckles et al., 2013).

Notably, Thaumarchaeota did not bloom during the 2008/09 austral summer, which most likely accounts for the low crenarchaeol abundance in CH10 surface sediments compared to CH07 (Figs. 2e and 5b). Since Thaumarchaeota are nitrifiers (Könneke et al., 2005; Wuchter et al., 2006), they should in principle have prospered on the ammonium released by biomass degradation resulting from the massive diatom bloom recorded in July–August 2008 (Barker et al., 2011). In fact, North Sea studies have shown that thaumarchaeotal blooms follow phytoplankton blooms in that setting (Wuchter et al., 2005; Pitcher et al., 2011a). However, in Lake Challa during the 2008/09 austral summer, Thaumarchaeota appear to have been outcompeted first by

GDGT-0 producing archaea, resulting in the high proportion of GDGT-0 in CH10 sediments (Fig. 5a), and perhaps subsequently by brGDGT-producing bacteria occupying a similar niche in the suboxic water column (Buckles et al., 2013, 2014a). Although little is known about the ecology or even identity of brGDGT-producing bacteria (Weijers et al., 2009; Sinninghe Damsté et al., 2011), the occurrence of a similar brGDGT peak in December 2006 (Sinninghe Damsté et al., 2009; Fig. 2c), i.e. following the austral winter diatom bloom of 2006 (Wolff et al., 2014), suggests that also brGDGT-producing bacteria may thrive on diatom degradation products. Abundances of total brGDGTs and crenarchaeol in monthly fluxes of settling particles do correlate ($r = 0.66$), indicating that the brGDGT-producing bacteria and Thaumarchaeota within the water column of Lake Challa require similar environmental and/or ecological conditions. This would fit with compound-specific carbon isotopic analyses on soils (Weijers et al., 2011; Opperman et al., 2011) which suggest that brGDGT producers are heterotrophic bacteria.

Microbiological analysis of suspended particulate matter (SPM) from Lake Challa collected in February 2010 (Buckles et al., 2013) yielded no evidence of methanogens or other anaerobic archaea in the upper 35 m of the water column, in line with the near-zero fluxes of GDGT-0 in settling particles trapped at this time (Fig. 2c). However, in SPM from anoxic waters deeper down, Buckles et al. (2013) found high concentrations of GDGT-0. Based on 16S rRNA sequence data, its source was identified as the uncultured archaeal group 1.2 (also named C3 by DeLong and Pace, 2001) and the "miscellaneous Crenarchaeota group" (MCG, also referred to as group 1.3; Inagaki et al., 2003). Presence of these archaeal sequences in the permanently stratified lower water column during a single sampling of SPM does not prove the origin of similar isoGDGT distributions in settling particles from the suboxic zone two years previously. Comparison with denaturing gradient gel electrophoresis (DGGE) performed on Lake Challa SPM taken in September 2007 (Sinninghe Damsté et al., 2009) does show that archaea in the anoxic water column also mostly fall in Group 1.2 and the MCG (MBG-C) group of the Crenarchaeota, as well as showing contributions from Halobacteriales of the Euryarchaeota. Nevertheless, given coincidence of the GDGT-0 maximum with

CPD
11, 1177–1218, 2015

the peak of the 2008 diatom bloom, and the position of the sediment trap in the sub-oxic water column, we tentatively infer that the GDGT-0 producers in Lake Challa are likely involved in the degradation of dead, settling diatoms as the austral winter bloom reaches its peak. Alternatively, as a result of the unusually high oxygen demand of the 2008 diatom bloom, the chemocline may have temporarily ascended. This could have resulted in the GDGT-0 producing archaea residing above the sediment trap and their signal captured by our analysis.

4.3 Effect of a soil-erosion event on the GDGT-producing community

The occurrence of a short-lived influx of allochthonous material in March–April 2008 provides a potential explanation for the change in the GDGT-producing community of Lake Challa that caused the dramatic shift in GDGT composition between CH07 and CH10 surface sediments.

Material settling in Lake Challa from March to May 2008 displayed a singularly large peak in the molar ratio of titanium to aluminium (Ti/Al; Fig. 2a), a tracer for the origin of detrital mineral sediment components (Weltje and Tjallingii, 2008; Wolff et al., 2014). This coincided with a peak in bulk flux (4.0–2.0 $g\,m^{-2}\,day^{-1}$), very low organic-matter content (3 % C_{org}; Fig. 2b), and local reports of the lake "turning brown", all pointing to enhanced allochthonous input to the lake triggered by the onset of the principal rain season that year (Fig. 2a). The likely source of this material is loose topsoil on and beyond the NW rim of Challa crater, mobilised during particularly intense precipitation and carried to the lake by the usually dry creek which breaches the rim there (Fig. 1). This particular precipitation event occurred after 10 consecutive months of drought (Fig. 2a; Table S3), which must have wilted the already sparse vegetation cover in that area and made significant soil erosion more likely. Notably, brGDGT distributions and abundances in particulate matter settling during these months were not discernibly affected by soil-derived brGDGTs, most probably due to the high background flux of lacustrine brGDGTs and the low organic matter content of the eroded soil (Buckles et al., 2014a; Table S3). If this soil-erosion event did cause the observed shift in Lake Challa's GDGT-producing community, its effect must have been indirect.

Nutrients triggering the annual diatom bloom in Lake Challa during austral winter are generally sourced from its anoxic, nutrient-rich lower water column by wind-driven seasonal mixing (Wolff et al., 2011, 2014; Barker et al., 2013). In the austral winter of 2008, seasonal mixing began already in June and re-establishment of stratification was slow (Wolff, 2012; Buckles et al., 2014a; Wolff et al., 2014). However, the massive diatom bloom of July–August 2008 (far larger than any other in the 4 year time series; Barker et al., 2011) peaked during the early months of deep seasonal mixing so the extended period of nutrient advection that year is unlikely to have been the main cause of this particularly abundant diatom bloom. We hypothesise that additional, soil-derived (micro-)nutrients delivered during intense rainfall between March and May 2008 may have been the primary driver for the unusually large diatom productivity later that year. Nutrients released by the decomposition of soil organic material in the lake would amplify the (annual) 2008 austral winter diatom bloom (Fig. 2b; Wolff et al., 2011). The delivery of large quantities of organic matter could result in higher ammonium, disturbing the competition of nitrifying archaea and bacteria. As nitrifying bacteria have a competitive advantage over nitrifying archaea at higher ammonium levels (Di et al., 2009) and vice versa (Martens-Habbena et al., 2009), increased ammonium could suppress Thaumarchaeota and its production of crenarchaeol and result in the absence of the quasi-annual thaumarchaeotal bloom in the 2008–2009 austral summer season. Considering that the coincident peak flux of GDGT-0 is especially clear in the IPL lipids, we infer that a certain (eury)archaeal community developed in the oxic/suboxic water layer below the euphotic zone, simultaneously with the diatoms in the epilimnion.

4.4 Connection of the BIT index to precipitation

Since soil-derived brGDGTs entering Lake Challa during March–May 2008 did not discernibly affect the brGDGT distributions and abundances in particulate matter settling at that time (Buckles et al., 2014a), the event is barely registered in the BIT index of those settling particles (Fig. 2f). Then how does this evidence support use of the BIT index as hydroclimatic proxy in this system (Verschuren et al., 2009)? We propose that in this relatively unproductive tropical lake system, episodic injection of extra nutrients derived from soils mobilized by intense precipitation creates a positive feedback loop leading to the suppression of Thaumarchaeota, via changes in the lake's planktonic and microbial communities. Variation in the relative proportions of crenarchaeol and brGDGTs in the 25 000 year, low-resolution record (Sinninghe Damsté et al., 2012a) had already indicated that variability in crenarchaeol is the main driver of BIT index changes in Lake Challa. Also in the high-resolution record studied here, BIT index values correlate (negatively) with the concentrations ($\mu g\,g^{-1}$ C_{org}) of crenarchaeol ($r = -0.69$) and its regioisomer ($r = -0.68$) but lacks a statistically significant correlation with brGDGT concentrations (Table S2). Thus, the hypothesized suppression of Thaumarchaeota following an event of intense precipitation increases the BIT index via its reduction of crenarchaeol deposition (cf. Fig. 5b). We postulate that the strongly seasonal nature of thaumarchaeotal production and its dependency on its suboxic niche in the water column leaves it more vulnerable to exceptional events.

Several other hypotheses can be put forward to explain the general match between the BIT index and seismic-reflection evidence in Lake Challa (Verschuren et al. (2009). First, lake-level fluctuation alters the relative volumes of the annually and infrequently mixed portions of the water column, thus changing the availability of niches favourable to either Thaumarchaeota or brGDGT-producing bacteria. For example, an increase in accommodation space for Thaumarchaeota in the suboxic zone when lake-level is high (cf. Sinninghe Damsté et al., 2012a) may result in conditions more favourable to lacustrine brGDGT production than to Thaumarchaeota, and vice versa.

More relevant at short time scales is the relationship between strong or prolonged dry winds during the austral winter season and reduced precipitation at Lake Challa (Wolff et al., 2011). Stronger wind and its lake-surface cooling result in deeper mixing, enhancing both the regeneration of nutrients from the lower water column to the photic zone as well as delaying the recovery of water-column stratification (Wolff et al., 2011). Since stronger austral-winter winds are associated with a weak southeasterly monsoon compromising the main rain season during March–May, dry years promote large diatom blooms that are followed by a greater proliferation of Thaumarchaeota and crenarchaeol production. As a result, dry years may tend to produce low BIT indices.

4.5 A high-resolution record of monsoon precipitation?

Wolff et al. (2011) produced a high-resolution record of inter-annual rainfall variation over the past 3000 years based on varve thickness variation in the same composite sediment sequence that we analysed at 1 cm resolution (Fig. 7a). Varve thickness in Lake Challa is mainly determined by the abundance of diatom frustules developing during the mixing season in austral winter; thus thicker varves were tied to stronger and more extended seasonal windy conditions associated with dry (La Niña) years. Although it was noted by Wolff et al. (2011) that this precipitation reconstruction corresponds with the findings of the low-resolution, 25 kyr BIT index record (Verschuren et al., 2009), here we find only a weak (negative) correlation ($r = -0.14$) between the high-resolution BIT index and integrated varve thickness per cm (Table S2; Fig. 7b). Since the varve thickness record has been shown to correspond well with El Niño/La Niña events spanning just 2 to 3 years, it seems likely that the wide variability seen in the BIT index record does not reflect the variability in crenarchaeol fluxes over 2–3 years (as observed in the sediment-trap record) sufficiently to work well as precipitation proxy at interannual timescale. However, on the decadal timescale the BIT index record average out the occurrence of multiple rainfall-driven “events”, such as the large influx of soil organic matter reported here, that affect local microbial community structure and therefore the balance of GDGTs deposited in sediments. In fact, the three most prominent negative excursions in our high-resolution BIT-index record match the timing of the three most prominent episodes of (multi-)decadal drought in equatorial East Africa over the past 250 years (Fig. 7b): the late-18th and earliest 19th century (Verschuren, 1999; Verschuren et al., 2000; Bessems et al., 2008); the late 19th century (Nicholson et al., 2012); and the mid-20th century (Verschuren et al., 1999; Ver-

CPD
11, 1177–1218, 2015

schuren, 2004). The BIT record also replicates the generally dry conditions during the 12th and 13th centuries and wetter conditions during the Little Ice Age known from elsewhere in the region (Verschuren, 2001, 2004). We therefore suggest that the BIT index should not be used as a precipitation proxy on the interannual timescale. Rather, one data point per decade seems sensible, with a five-point moving average (Fig. 7b) providing a robust reconstruction of longer-term dry/wet trends.

Finally, we note that our reconstruction of monsoon precipitation using the BIT index of Lake Challa sediments is contingent upon site-specific conditions: the permanent stratification of its lower water column, dominance of in situ produced brGDGTs, strong seasonality in rainfall, drought and wind, and the resulting intermittent fluxes of soil mobilised from a semi-arid landscape. Since these peculiarities make the BIT index an effective precipitation proxy at Lake Challa, its application in other lakes is only recommended when the degree of in situ brGDGT production and factors controlling the productivity of Thaumarchaeota have been identified.

5 Conclusions

Loose soil material transported to Lake Challa by intense precipitation between March and May 2008 stimulated aquatic productivity and set in motion a sequence of events which shifted the composition of GDGTs exported to profundal bottom sediments. It included a suppression of the seasonal Thaumarchaeota, and thus reduced the production of crenarchaeol reflected in the BIT index of settling particles and profundal sediments. Similarly, variation in the sedimentary BIT index over the past 2200 years results from fluctuations in crenarchaeol production against a background of high in situ brGDGT production. Integrated over 10 year intervals, the magnitude of this longer-term BIT-index variation is smaller than that observed in the 45 month long time series of settling particles, but similar to that observed between two sets of recent surface sediments collected before and after the episode of Thaumarchaeota suppression.

CPD
11, 1177–1218, 2015

Decadally-averaged BIT index values correlate weakly with the annually-resolved precipitation reconstruction for the Lake Challa region based on varve thickness, but capture the three most prominent known episodes of prolonged regional drought of the past 200 years. This suggests that, while rainfall-triggered events of Thaumarchaeota suppression may occur rather infrequently at the inter-annual time scale, their probability of occurrence is reduced during longer episodes of relative drought, and enhanced during longer episodes of higher average rainfall, such that a temporally integrated BIT index record reflects multi-decadal trends in rainfall. Marked decadal maxima and minima in the sedimentary BIT index are further smoothed by integration over longer intervals, such as the ca. 40 year intervals represented by each data point in the 25 000 year BIT index record (Verschuren et al., 2009; Sinninghe Damsté et al., 2012a). We conclude that the BIT index is a reliable precipitation proxy, at least in the Lake Challa system and on (multi-)decadal and longer time scales. However, prior to application elsewhere we recommend ascertaining the local situation of lacustrine brGDGT production and of variables affecting the productivity of Thaumarchaeota.

The Supplement related to this article is available online at doi:10.5194/cpd-11-1177-2015-supplement.

Acknowledgements. We thank all those who provided fieldwork support, notably C. Mukhwana Oluseno, and J. Blokker, as well as J. Ossebaar for laboratory assistance. We thank the Kenyan Ministry of Agriculture for monthly precipitation data from the Challa Agricultural Station, A. Hemp for air temperature data and B. Plessen for organic carbon data from the sediment core. The research leading to the results presented here received funding from the European Research Council under the European Union's Seventh Framework Programme (*FP7/2007–2013)*/ERC grant agreement n° *226 600*. J. W. H. Weijers acknowledges a Veni grant from the Netherlands Organisation for Scientific Research (NWO). Fieldwork was conducted with support from the Research Foundation Flanders (FWO) and under permit 13/001/11C of the Kenyan Ministry of Education, Science and Technology to D. Verschuren.

References

Barker, P. A., Hurrell, E. R., Leng, M. J., Wolff, C., Cocquyt, C., Sloane, H. J. and Verschuren, D.: Seasonality in equatorial climate over the last 25 000 years revealed by oxygen isotope records from Mount Kilimanjaro, Geology, 39, 1111–1114, 2011.

Barker, P. A., Hurrell, E. R., Leng, M. J., Plessen, B., Wolff, C., Conley, D. J., Keppens, E., Milne, I., Cumming, B. F., Laird, K. R., Kendrick, C. P., Wynn, P. M., and Verschuren, D.: Carbon cycling within an East African lake revealed by the carbon isotope composition of diatom silica: a 25 ka record from Lake Challa, Mt. Kilimanjaro, Quaternary Sci. Rev., 66, 55–63, 2013.

Bessems, I., Verschuren, D., Russell, J. M., Hus, J., Mees, F., and Cumming, B. F.: Palaeolimnological evidence for widespread late 18th century drought across equatorial East Africa, Palaeogeogr. Palaeocl., 259, 107–120, 2008.

Blaga, C. I., Reichart, G. J., Heiri, O., and Sinninghe Damsté J. S.: Tetraether membrane lipid distributions in water-column particulate matter and sediments: a study of 47 European lakes along a north–south transect, J. Paleolimnol., 41, 523–540, 2009.

Blaauw, M., van Geel, B., Kristen, I., Plessen, B., Lyaruu, A., Engstrom, D. R., van der Plicht, J., and Verschuren, D.: High-resolution ^{14}C dating of a 25 000 year lake-sediment record from equatorial East Africa, Quaternary Sci. Rev., 30, 3043–3059, 2011.

Bligh, E. G. and Dyer, W. J.: A rapid method of total lipid extraction and purification, Can. J. Biochem. Phys., 37, 911–917, 1959.

Brochier-Armanet, C., Boussau, B., Gribaldo, S., and Forterre, P.: Mesophilic crenarchaeota: proposal for a third archaeal phylum, the Thaumarchaeota, Nature Rev. Microbiol., 6,245–252, 2008.

Buckles, L. K., Villanueva, L., Weijers, J. W. H., Verschuren, D., and Sinninghe Damsté J. S.: Linking isoprenoidal GDGT membrane-lipid distributions with gene abundances of ammonia-oxidising Thaumarchaeota and uncultured crenarchaeotal groups in the water column of a tropical lake (Lake Challa, East Africa), Environ. Microbiol., 15, 2445–2462, 2013.

Buckles, L. K., Weijers, J. W. H., Verschuren, D., and Sinninghe Damsté J. S.: Sources of core and intact branched tetraether membrane lipids in the lacustrine environment: anatomy of Lake Challa and its catchment, equatorial East Africa, Geochim. Cosmochim. Ac., 140, 106–126, 2014a.

Buckles, L. K., Weijers, J. W. H., Tran, X.-M., Waldron, S., and Sinninghe Damsté, J. S.: Provenance of tetraether membrane lipids in a large temperate lake (Loch Lomond, UK): implications for glycerol dialkyl glycerol tetraether (GDGT)-based palaeothermometry, Biogeosciences, 11, 5539–5563, doi:10.5194/bg-11-5539-2014, 2014b.

Dean, W. E.: Determination of carbonate and organic matter in calcareous sediments and sedimentary rocks by loss on ignition: comparison with other methods, J. Sediment. Petrol., 44, 242–248, 1974.

DeLong, E. F. and Pace, N. R.: Environmental diversity of bacteria and archaea, Syst. Biol., 50, 470–478, 2001.

Di, H. J., Cameron, K. C., Shen, J. P., Winefield, C. S., O'Callaghan, M., Bowatte, S., and He, J. Z.: Nitrification driven by bacteria and not archaea in nitrogen-rich grassland soils, Nat. Geosci., 2, 621–624, 2009.

Harvey, H. R., Fallon, R. D., and Patton, J. S.: The effect of organic matter and oxygen on the degradation of bacterial membrane lipids in marine sediments, Geochim. Cosmochim. Ac., 50, 795–804, 1986.

Hopmans, E. C., Weijers, J. W. H., Schefuß, E., Herfort, L., Sinninghe Damsté J. S., and Schouten, S.: A novel proxy for terrestrial organic matter in sediments based on branched and isoprenoid tetraether lipids, Earth Planet. Sc. Lett., 224, 107–116, 2004.

Huguet, C., Hopmans, E. C., Febo-Ayala, W., Thompson, D. H., Sinninghe Damsté J. S., and Schouten, S.: An improved method to determine the absolute abundance of glycerol dibiphytanyl glycerol tetraether lipids, Org. Geochem., 37, 1036–1041, 2006.

Huguet, C., Martens-Habbena, W., Urakawa, H., Stahl, D. A., and Ingalls, A. E.: Comparison of extraction methods for quantitative analysis of core and intact polar glycerol dialkyl glycerol tetraethers (GDGTs) in environmental samples, Limnol. Oceanogr.-Meth., 8, 127–145, 2010.

Inagaki, F., Suzuki, M., Takai, K., Oida, H., Sakamoto, T., Aoki, K., Nealson, K. H., and Horikoshi, K.: Microbial communities associated with geological horizons in coastal subseafloor sediments from the Sea of Okhotsk, Appl. Environ. Microb., 69, 7224–7235, 2003.

Kim, J. H., Schouten, S., Hopmans, E. C., Donner, B., and Sinninghe Damsté J. S.: Global sediment core-top calibration of the TEX_{86} paleothermometer in the ocean, Geochim. Cosmochim. Ac., 72, 1154–1173, 2008.

Kim, J., van der Meer, J., Schouten, S., Helmke, P., Willmott, V., Sangiorgi, F., Koç N., Hopmans, E. C., and Damsté J. S. S.: New indices and calibrations derived from the distribution

of crenarchaeal isoprenoid tetraether lipids: implications for past sea surface temperature reconstructions, Geochim. Cosmochim. Ac., 74, 4639–4654, 2010.
Könneke M., Bernhard, A. E., de la Torre, J. R., Walker, C. B., Waterbury, J. B., and Stahl, D. A.: Isolation of an autotrophic ammonia-oxidizing marine archaeon, Nature, 437, 543–546, 2005.
Kristen, I.: Investigations on Rainfall Variability During the Late Quarternary Based on Geochemical Analyses of Lake Sediments From Tropical and Subtropical Southern Africa, Ph.D. thesis, Universität Potsdam, Potsdam : Deutsches GeoForschungsZentrum GFZ, doi:10.2312/GFZ.b103-10018, 2009.
Leininger, S., Urich, T., Schloter, M., Schwark, L., Qi, J., Nicol, G. W., Prosser, J. I., Schuster, S. C., and Schleper, C.: Archaea predominate among ammonia-oxidizing prokaryotes in soils, Nature, 442, 806–809, 2006.
Lengger, S. K., Hopmans, E. C., Sinninghe Damsté J. S., and Schouten, S.: Comparison of extraction and work up techniques for analysis of core and intact polar tetraether lipids from sedimentary environments, Org. Geochem., 47, 34–40, 2012.
Lipp, J. S. and Hinrichs, K.: Structural diversity and fate of intact polar lipids in marine sediments, Geochim. Cosmochim. Ac., 73, 6816–6833, 2009.
Lipp, J. S., Morono, Y., Inagaki, F., and Hinrichs, K. U.: Significant contribution of Archaea to extant biomass in marine subsurface sediments, Nature, 454, 991–994, 2008.
Liu, X., Leider, A., Gillespie, A., Groeger, J., Versteegh, G. J. M., and Hinrichs, K.: Identification of polar lipid precursors of the ubiquitous branched GDGT orphan lipids in a peat bog in Northern Germany, Org. Geochem., 41, 653–660, 2010.
Loomis, S. E., Russell, J. M., and Sinninghe Damsté J. S.: Distributions of branched GDGTs in soils and lake sediments from western Uganda: implications for a lacustrine paleothermometer, Org. Geochem., 42, 739–751, 2011.
Loomis, S. E., Russell, J. M., Ladd, B., Street-Perrott, F. A., and Sinninghe Damsté J. S.: Calibration and application of the branched GDGT temperature proxy on East African lake sediments, Earth Planet. Sc. Lett., 357–358, 277–288, 2012.
Mitchell, J. F. B.: Can we believe predictions of climate change?, Q. J. Roy. Meteor. Soc., 130, 2341–2360, 2004.
Martens-Habbena, W., Berube, P. M., Urakawa, H., de la Torre, J. R., and Stahl, D. A.: Ammonia oxidation kinetics determine niche separation of nitrifying archaea and bacteria, Nature, 461, 976–979, 2009.

CPD
11, 1177–1218, 2015

Short-term variability in the sedimentary BIT index of Lake Challa

L. K. Buckles et al.

Nicholson, S. E., Klotter, D., and Dezfuli, A. K.: Spatial reconstruction of semi-quantitative precipitation fields over Africa during the nineteenth century from documentary evidence and gauge data, Quaternary Res., 78, 13–23, 2012.
Oppermann, B. I., Michaelis, W., Blumenberg, M., Frerichs, J., Schulz, H. M., Schippers, A., Beaubien, S. E., and Krüger M.: Soil microbial community changes as a result of long-term exposure to a natural CO_2 vent, Geochim. Cosmochim. Ac., 74, 2697–2716, 2010.
Payne, B. R.: Water balance of Lake Chala and its relation to groundwater from tritium and stable isotope data, J. Hydrol., 11, 47–58, 1970.
Pitcher, A., Villanueva, L., Hopmans, E. C., Schouten, S., Reichart, G.-J., and Sinninghe Damsté J. S.: Niche segregation of ammonia-oxidizing archaea and annamox bacteria in the Arabian Sea oxygen minimum zone, ISME J., 5, 1896–1904, 2011.
Pitcher, A., Hopmans, E. C., Mosier, A. C., Park, S., Rhee, S., Francis, C. A., Schouten, S., and Sinninghe Damsté J. S.: Core and intact polar glycerol dibiphytanyl glycerol tetraether lipids of ammonia-oxidizing archaea enriched from marine and estuarine sediments, Appl. Environ. Microb., 77, 3468–3477, 2011.
Powers, L. A., Johnson, T. C., Werne, J. P., Castanada, I. S., Hopmans, E. C., Sinninghe Damsté, J. S., and Schouten, S.: Large temperature variability in the southern African tropics since the Last Glacial Maximum, Geophys. Res. Lett., 32, L08706, 2005.
Rossel, P. E., Lipp, J. S., Fredricks, H. F., Arnds, J., Boetius, A., Elvert, M., and Hinrichs, K.: Intact polar lipids of anaerobic methanotrophic archaea and associated bacteria, Org. Geochem., 39, 992–999, 2008.
Schouten, S., Hopmans, E. C., Schefuss, E., and Sinninghe Damsté J. S.: Distributional variations in marine crenarchaeotal membrane lipids: a new tool for reconstructing ancient sea water temperatures?, Earth Planet. Sc. Lett., 204, 265–274, 2002.
Schouten, S., Huguet, C., Hopmans, E. C., Kienhuis, M. V. M., and Sinninghe Damsté J. S.: Analytical methodology for TEX_{86} paleothermometry by high-performance liquid chromatography/atmospheric pressure chemical ionization-mass spectrometry, Anal. Chem., 79, 2940–2944, 2007.
Schubotz, F., Wakeham, S. G., Lipp, J. S., Fredricks, H. F., and Hinrichs, K.: Detection of microbial biomass by intact polar membrane lipid analysis in the water column and surface sediments of the Black Sea, Environ. Microbiol., 11, 2720–2734, 2009.
Sinninghe Damsté, J. S., Schouten, S., Hopmans, E. C., van Duin, A. C. T., and Geenevasen, J. A. J.: Crenarchaeol: the characteristic core glycerol dibiphytanyl glycerol

CPD
11, 1177–1218, 2015

tetraether membrane lipid of cosmopolitan pelagic crenarchaeota, J. Lipid Res., 43, 1641–1651, 2002.

Sinninghe Damsté, J. S., Ossebaar, J., Abbas, B., Schouten, S., and Verschuren, D.: Fluxes and distribution of tetraether lipids in an equatorial African lake: constraints on the application of the TEX_{86} palaeothermometer and BIT index in lacustrine settings, Geochim. Cosmochim. Ac., 73, 4232–4249, 2009.

Sinninghe Damsté, J. S., Ossebaar, J., Schouten, S., and Verschuren, D.: Distribution of tetraether lipids in the 25 ka sedimentary record of Lake Challa: extracting reliable TEX_{86} and MBT/CBT palaeotemperatures from an equatorial African lake, Quaternary Sci. Rev., 50, 43–54, 2012.

Spang, A., Hatzenpichler, R., Brochier-Armanet, C., Rattei, T., Tischler, P., Spieck, E., Streit, W., Stahl, D. A., Wagner, M., and Schleper, C.: Distinct gene set in two different lineages of ammonia-oxidizing archaea supports the phylum thaumarchaeota, Trends Microbiol., 18, 331–340, 2010.

Tierney, J. E. and Russell, J. M.: Distributions of branched GDGTs in a tropical lake system: implications for lacustrine application of the MBT/CBT paleoproxy, Org. Geochem., 40, 1032–1036, 2009.

Tierney, J. E., Russell, J. M., Sinninghe Damsté J. S., Huang, Y., and Verschuren, D.: Late Quaternary behavior of the East African monsoon and the importance of the Congo Air Boundary, Quaternary Sci. Rev., 30, 798–807, 2011.

Tierney, J. E., Schouten, S., Pitcher, A., Hopmans, E. C., and Sinninghe Damsté J. S.: Core and intact polar glycerol dialkyl glycerol tetraethers (GDGTs) in Sand Pond, Warwick, Rhode Island (USA): insights into the origin of lacustrine GDGTs, Geochim. Cosmochim. Ac., 77, 561–581, 2012.

Tierney, J. E., Smerdon, J. E., Anchukaitis, K. J., and Seager, R.: Multidecadal variability in East African hydroclimate controlled by the Indian Ocean, Nature, 493, 389–392, 2013.

Utermöhl, H.: Neue Wege in der quantitativen Erfassung des Planktons, Verh. Int. Ver. Theor. Angew. Limnol., 5, 567–596, 1931.

Verschuren, D.: Influence of depth and mixing regime on sedimentation in a small, fluctuating tropical soda lake, Limnol. Oceanogr., 44, 1103–1113, 1999.

Verschuren, D.: Reconstructing fluctuations of a shallow East African lake during the past 1800 yrs from sediment stratigraphy in a submerged crater basin, J. Paleolimnol., 25, 297–311, 2001.

Verschuren, D.: Decadal and century-scale climate variability in tropical Africa during the past 2000 years, in: Past Climate Variability through Europe and Africa, volume 6, edited by: Battarbee, R. W., Gasse, F., and Stickley, C. E., Springer, Dordrecht, the Netherlands, 139–158, 2004.

Verschuren, D., Tibby, J., Leavitt, P. R., and Roberts, C. N.: The environmental history of a climate-sensitive lake in the former “White Highlands” of central Kenya, Ambio, 28, 494–501, 1999.

Verschuren, D., Laird, K. R., and Cumming, B. F.: Rainfall and drought in equatorial east Africa during the past 1100 years, Nature, 403, 410–414, 2000.

Verschuren, D., Sinninghe Damsté, J. S., Moernaut, J., Kristen, I., Blaauw, M., Fagot, M., Haug, G. H., and CHALLACEA project members: Half-precessional dynamics of monsoon rainfall near the East African Equator, Nature, 462, 637–641, 2009.

Wang, H., Liu, W., Zhang, C. L., Liu, Z., and He, Y.: Branched and isoprenoid tetraether (BIT) index traces water content along two marsh-soil transects surrounding Lake Qinghai: implications for paleo-humidity variation, Org. Geochem., 59, 75–81, 2013.

Weltje, G. J. and Tjallingii, R.: Calibration of XRF core scanners for quantitative geochemical logging of soft sediment cores: theory and application, Earth Planet. Sc. Lett., 274, 423–438, 2008.

Weijers, J. W. H., Schouten, S., van der Linden, M., van Geel, B., and Sinninghe Damsté J. S.: Water table related variations in the abundance of intact archaeal membrane lipids in a Swedish peat bog, FEMS Microbiol. Lett., 239, 51–56, 2004.

Weijers, J. W. H., Schouten, S., Hopmans, E. C., Geenevasen, J. A. J., David, O. R. P., Coleman, J. M., Pancost, R. D., and Sinninghe Damsté J. S.: Membrane lipids of mesophilic anaerobic bacteria thriving in peats have typical archaeal traits, Environ. Microbiol., 8, 648–657, 2006.

Weijers, J. W. H., Schouten, S., Schefuss, E., Schneider, R. R., and Sinninghe Damsté J. S.: Disentangling marine, soil and plant organic carbon contributions to continental margin sediments: a multi-proxy approach in a 20 000 year sediment record from the Congo deep-sea fan, Geochim. Cosmochim. Ac., 73, 119–132, 2009.

Wolff, C.: East African Monsoon Variability Since the Last Glacial, Ph.D. thesis, Deutsches GeoForschungsZentrum GFZ, Potsdam, 2012.

Wolff, C., Haug, G. H., Timmermann, A., Sinninghe Damsté J. S., Brauer, A., Sigman, D. M., Cane, M. A., and Verschuren, D.: Reduced interannual rainfall variability in East Africa during the Last Ice Age, Science, 333, 743–747, 2011.

Wolff, C., Kristen-Jenny, I., Schettler, G., Plessen, B., Meyer, H., Dulski, P., Naumann, R., Brauer, A., Verschuren, D., and Haug, G. H.: Modern seasonality in Lake Challa (Kenya/Tanzania) and its sedimentary documentation in recent lake sediments, Limnol. Oceanogr., 59, 621–1636, 2014.

Woltering, M., Werne, J. P., Kish, J. L., Hicks, R., Sinninghe Damsté J. S., and Schouten, S.: Vertical and temporal variability in concentration and distribution of thaumarchaeotal tetraether lipids in Lake Superior and the implications for the application of the TEX_{86} temperature proxy, Geochim. Cosmochim. Ac., 87, 136–153, 2012.

Zhang, Y. G., Zhang, C. L., Liu, X., Li, L., Hinrichs, K., and Noakes, J. E.: Methane Index: a tetraether archaeal lipid biomarker indicator for detecting the instability of marine gas hydrates, Earth Planet. Sc. Lett., 307, 525–534, 2011.

CPD
11, 1177–1218, 2015

Title Page
Abstract | Introduction
Conclusions | References
Tables | Figures
◀| |▶
◀ ▶
Back | Close
Full Screen / Esc
Printer-friendly Version
Interactive Discussion

Table 1. Mean ($\pm\sigma$) GDGT distributions and indices in CH10 and CH07 surface sediments. CH07 sediment data are collated from Sinninghe Damsté et al. (2009) and CH10 sediment data are collated from Buckles et al. (2014a).

	Depth interval (cm)	No. of cores	Water depth (m)		GDGT-I ($\mu g\,g^{-1}$ dry wt.)	GDGT-V ($\mu g\,g^{-1}$ dry wt.)	Σ[brGDGTs] ($\mu g\,g^{-1}$ dry wt.)	BIT	MBT	DC	
CH10	0–1	7	68–92	IPL	14.5 ($\pm$5.3)	0.3 ($\pm$0.5)	2.2 ($\pm$1.1)	0.90 ($\pm$0.10)	0.34 ($\pm$0.06)	0.15 ($\pm$0.01)	
				CL	8.7 ($\pm$3.2)	1.2 ($\pm$1.5)	8.5 ($\pm$2.0)	0.87 ($\pm$0.13)	0.36 ($\pm$0.06)	0.17 ($\pm$0.02)	
CH07	0–1	1	94	CL	5.1	7.4	6.5	0.50	n.m.[2]	n.m.	
	Depth interval (cm)	No. of cores	Water depth (m)		f[GDGT-I][3]	f[GDGT-II]	f[GDGT-III]	f[GDGT-IV]	f[GDGT-V]	f[GDGT-V′]	f[ΣbrGDGTs]
CH10	0–1	7	68–92	IPL	0.85 ($\pm$0.10)	0.00 ($\pm$0.00)	0.00 ($\pm$0.00)	0.00 ($\pm$0.00)	0.02 ($\pm$0.02)	0.00 ($\pm$0.00)	0.12 ($\pm$0.07)
				CL	0.49 ($\pm$0.13)	0.01 ($\pm$0.01)	0.01 ($\pm$0.01)	0.01 ($\pm$0.01)	0.07 ($\pm$0.08)	0.00 ($\pm$0.00)	0.42 ($\pm$0.04)
CH07	0–1	1	94	CL	0.25	0.02	0.06	0.02	0.32	0.01	0.32

[1] summed GDGTs VI, VII and VIII.
[2] n.m. = not measured.
[3] f[GDGT] represents fractional abundances of total GDGTs.

CPD
11, 1177–1218, 2015

Short-term variability in the sedimentary BIT index of Lake Challa

L. K. Buckles et al.

CPD
11, 1177–1218, 2015

Table 2. Fluxes and indices of GDGTs in settling particles throughout the estimated deposition periods of CH10 and CH07 surface sediments. GDGT data from 18 November 2006–1 December 2007 is collated from Sinninghe Damsté et al. (2009) and from 31 December 2007–31 August 2010 is collated from Buckles et al. (2014a).

Settling particles	Deployment date	Collection date	C_{org} (%)	Bulk flux ($g\,m^{-2}\,day^{-1}$)	GDGT-I ($\mu g\,m^{-2}\,day^{-1}$)		GDGT-V ($\mu g\,m^{-2}\,day^{-1}$)		Σ[brGDGTs][1] ($\mu g\,m^{-2}\,day^{-1}$)		BIT		MBT		DC	
					IPL	CL	IPL	CL	IPL	CL	IPL	CL	IPL	CL	IPL	CL
2008–2010 (CH10)	30 Jan 2008	30 Jan 2010	12.5	1.3	1.3	0.3	0.1	0.2	0.4	1.6	0.86	0.86	0.29	0.28	0.17	0.20
2006–2007 (CH07)	18 Nov 2006	24 Aug 2007	18.1	1.5	n.m.[2]	0.4	n.m.	2.3	n.m.	2.3	n.m.	0.50	n.m.	0.25	n.m.	0.18

[1] summed GDGTs VI(b, c), VII(b, c) & VIII(b, c).
[2] n.m. = not measured.

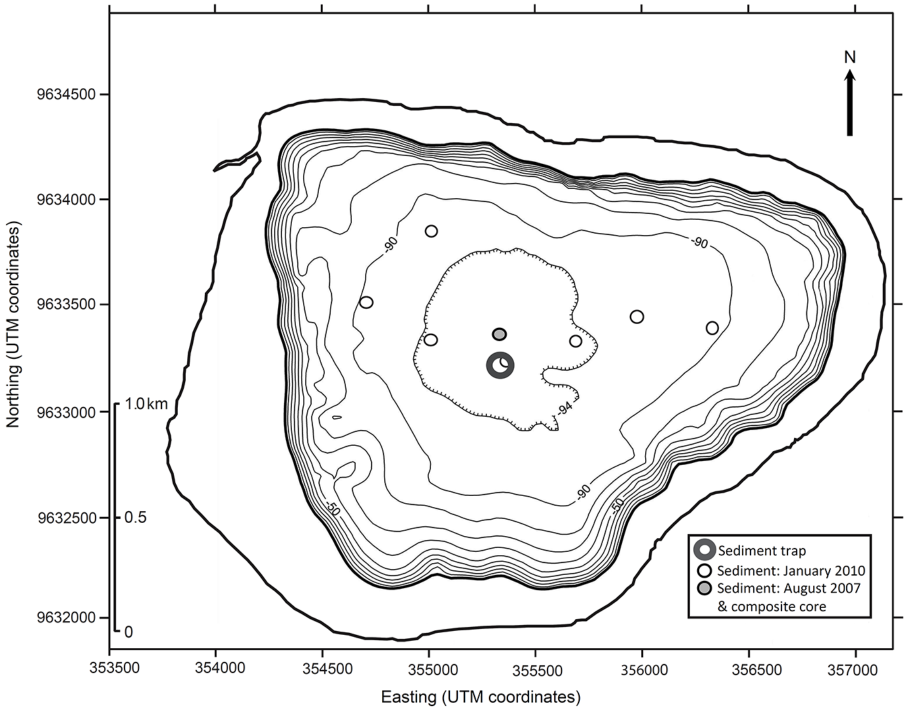

Figure 1. Map of Lake Challa with bathymetry and sampling sites indicated; scale is in the Universal Transverse Mercator (UTM) global coordinate system. The outermost bold black line denotes the catchment area boundary.

CPD
11, 1177–1218, 2015

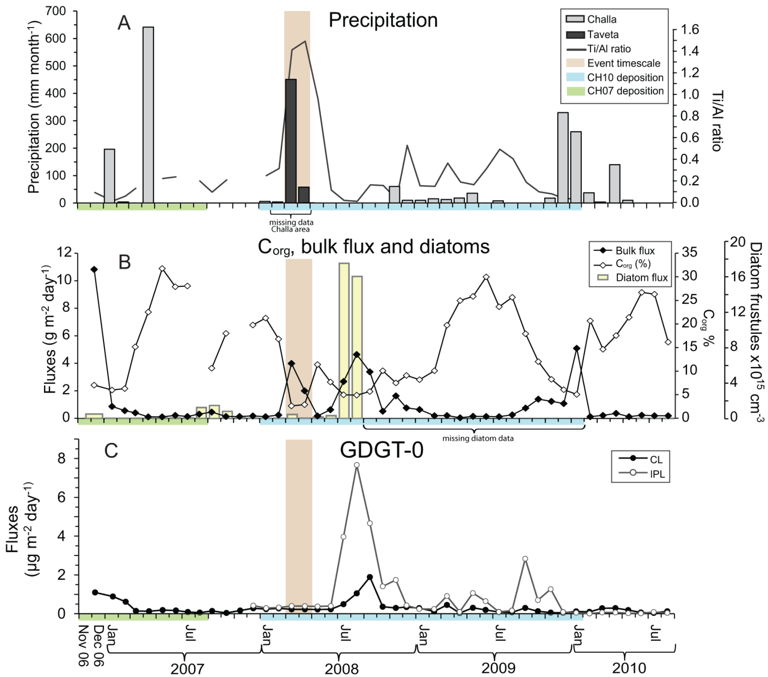

Figure 2. Fluxes and GDGT parameters of approximately monthly sediment-trap samples of settling particles, from 18 November 2006 to 31 August 2010. **(a)** Monthly precipitation at a Kenya government agricultural station immediately north of Lake Challa (cf. Buckles et al., 2014a) and the Ti/Al ratios of settling mineral particles (from Wolff et al., 2014). **(b)** Fluxes of bulk sedimenting particles and diatoms, and bulk percentage organic carbon (% C_{org}) content. Fluxes of **(c)** IPL and CL GDGT-0, **(d)** IPL and CL brGDGTs **(e)** IPL and CL crenarchaeol (GDGT-V) and **(f)** IPL and CL BIT index, with dashed horizontal lines representing the CL BIT indices of surface sediment deposited over those time periods. In **(c–f)**, data from 18 November 2006 to 1 December 2007 is by Sinninghe Damsté et al. (2009) and data from the following months until 31 August 2010 are by Buckles et al. (2014a).

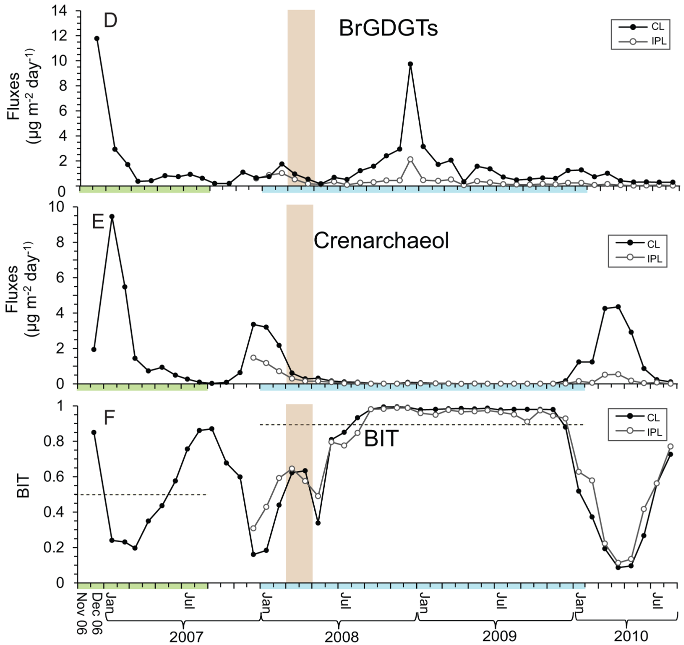

Figure 2. Continued.

CPD
11, 1177–1218, 2015

Short-term variability in the sedimentary BIT index of Lake Challa

L. K. Buckles et al.

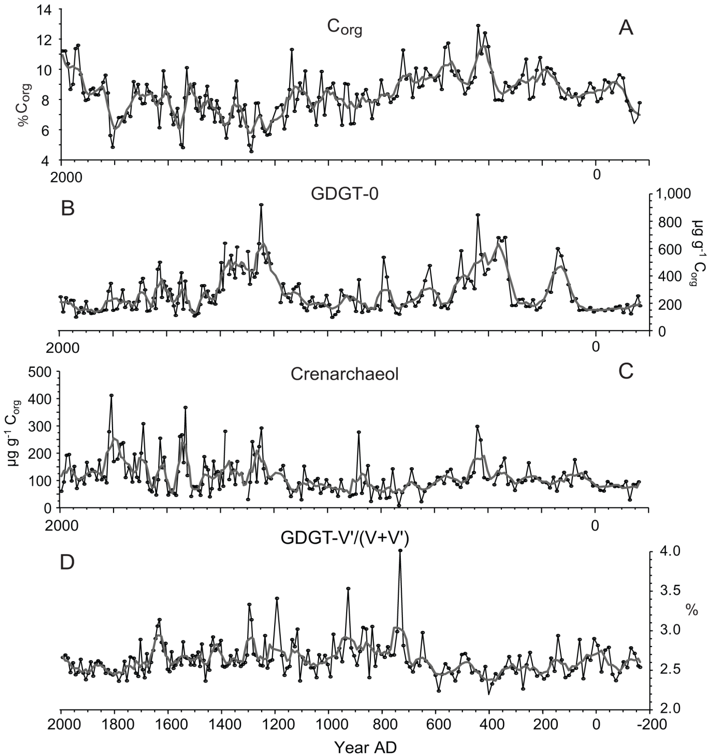

Figure 3. Bulk and GDGT parameters in the 213 cm long Lake Challa sediment sequence against years AD. **(a)** % C_{org}, **(b)** GDGT-0 abundance, **(c)** crenarchaeol (GDGT-V) abundance, **(d)** the percentage of crenarchaeol regioisomer with respect to crenarchaeol, **(e)** summed brGDGT abundance, and **(f)** BIT index. Points connected by a thin line represent raw data and the thicker black lines denote 5-point running averages. Missing data for GDGT abundances are due to gaps in % C_{org} measurement. **(g)** Comparison of 4 averaged 1 cm sections of the BIT index from the 213 cm core against integrated 4 cm sections of the same core analysed earlier by Verschuren et al. (2009).

CPD
11, 1177–1218, 2015

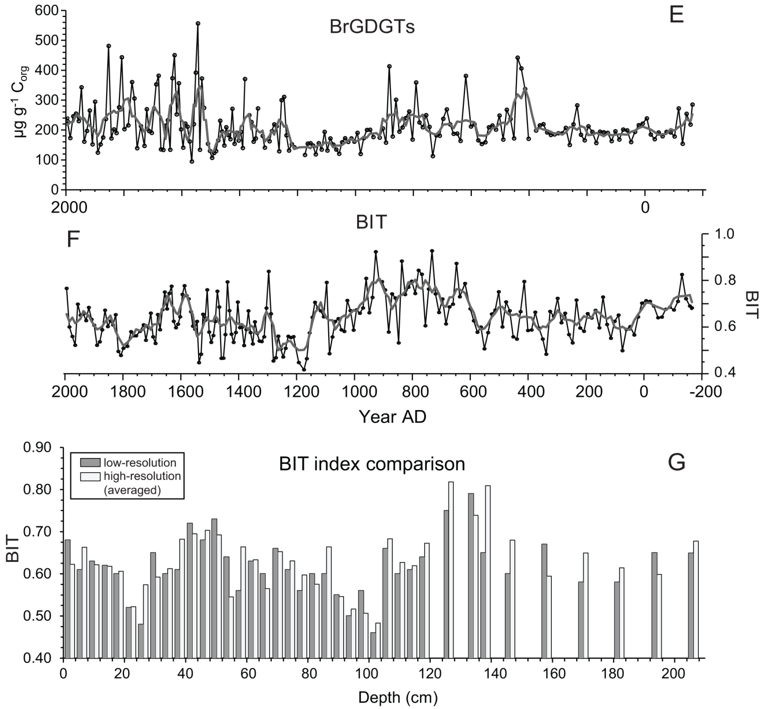

Figure 3. Continued.

CPD
11, 1177–1218, 2015

Short-term variability in the sedimentary BIT index of Lake Challa

L. K. Buckles et al.

Title Page
Abstract | Introduction
Conclusions | References
Tables | Figures
◀| |▶
◀ ▶
Back | Close
Full Screen / Esc
Printer-friendly Version
Interactive Discussion

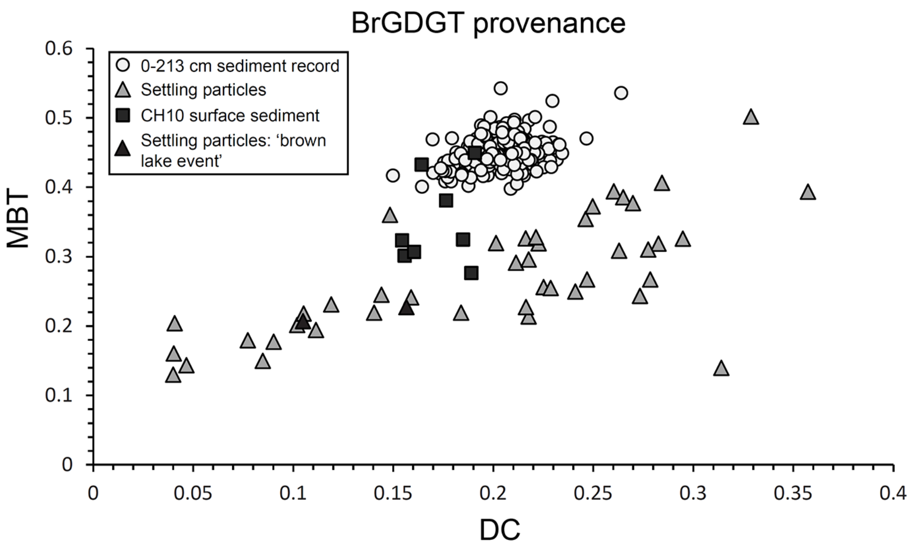

Figure 4. MBT vs. DC plot for the 0–213 cm sediment record (circles), for CH10 surface sediments (squares) from Buckles et al. (2014a), and settling particles (triangles; data from 18 November 2006 to 1 December 2007 are by Sinninghe Damsté et al., 2009 and data from the following months until 31 August 2010 are by Buckles et al., 2014a). Black triangles represent settling particles from March and April 2008, when the lake was reported turning brown.

CPD
11, 1177–1218, 2015

Short-term variability in the sedimentary BIT index of Lake Challa

L. K. Buckles et al.

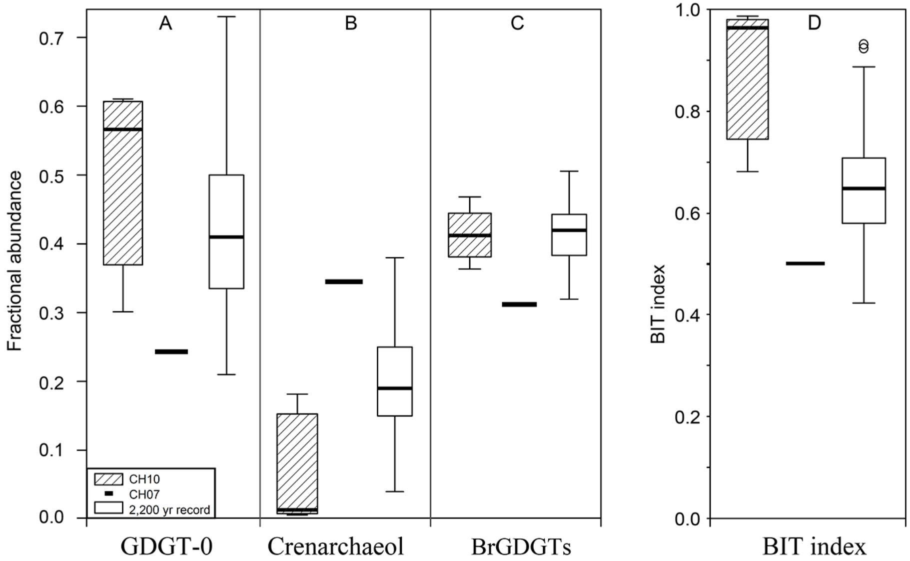

Figure 5. Boxplot of fractional abundances of **(a)** CL GDGT-0, **(b)** CL crenarchaeol, **(c)** CL summed brGDGTs and **(d)** of the BIT index, for respectively surface sediments CH10 ($n = 7$, 0–1 cm depth) collated from Buckles et al. (2014a), CH07 collated from Sinninghe Damsté et al. (2009) and the 2200 year sediment record (0–213 cm depth at 1 cm resolution, where 1 cm represents on average 10.4 years of deposition). Note that surface sediments represent 2–3 years of deposition. The box corresponds to the interquartile range and the whiskers extend to 1.5 times the length of the box (unless the full range of data is smaller than this); outliers are defined here as being outside the maximum extent of the whiskers. The black horizontal line inside the box represents the median.

CPD
11, 1177–1218, 2015

Short-term variability in the sedimentary BIT index of Lake Challa

L. K. Buckles et al.

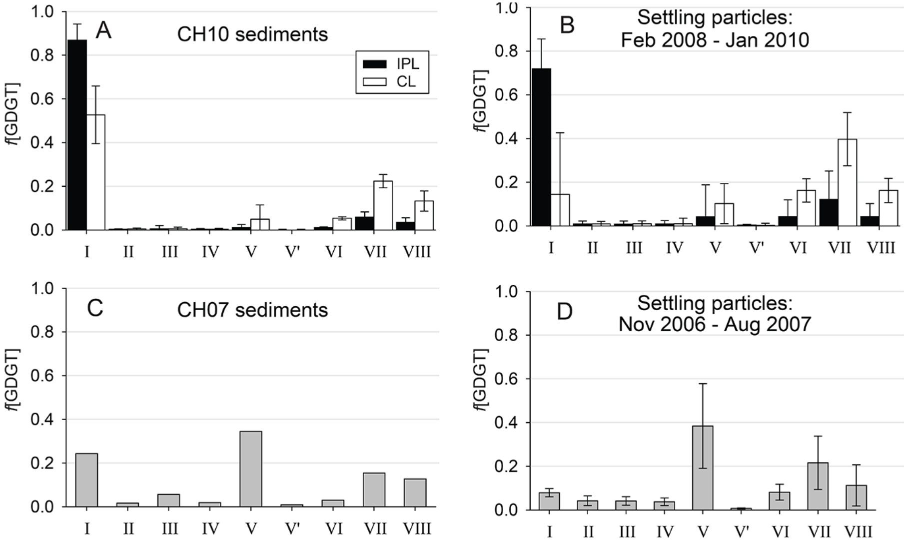

Figure 6. IPL and CL GDGT distributions from surface sediments **(a)** CH10 from Buckles et al. (2014a) with **(b)** corresponding weighted average IPL and CL GDGT distributions from summed fluxes of settling particles between 30 January 2008 and 30 January 2010, also from Buckles et al. (2014a). **(c)** CL GDGT distributions from surface sediment CH07 from Sinninghe Damsté et al. (2009) and **(d)** corresponding weighted average CL GDGT distributions from summed fluxes of settling particles between 18 November 2006 and 24 August 2007.

CPD
11, 1177–1218, 2015

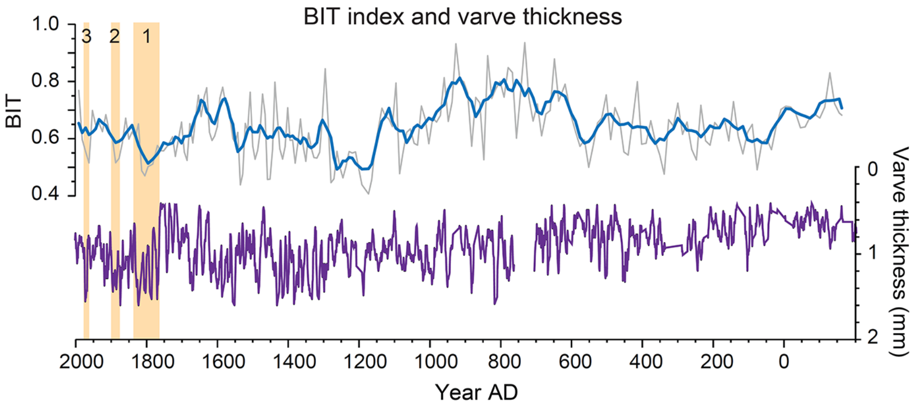

Figure 7. (a) BIT index in the 2200 year sediment record, where grey lines represent raw data and the blue line a 5-point running average. **(b)** A 7-point running average of varve thickness from Wolff et al. (2011). Orange shaded bars highlight recent periods of drought in East Africa: (1) 1760–1840 (Verschuren et al., 2000; Bessems et al., 2008), (2) 1880–1900 (Nicholson et al., 2012), and (3) spread over drought years 1964–1967, 1972–1973 and 1975–1976 (Verschuren et al., 1999; Verschuren, 2004).

CPD
11, 1177–1218, 2015

Short-term variability in the sedimentary BIT index of Lake Challa

L. K. Buckles et al.

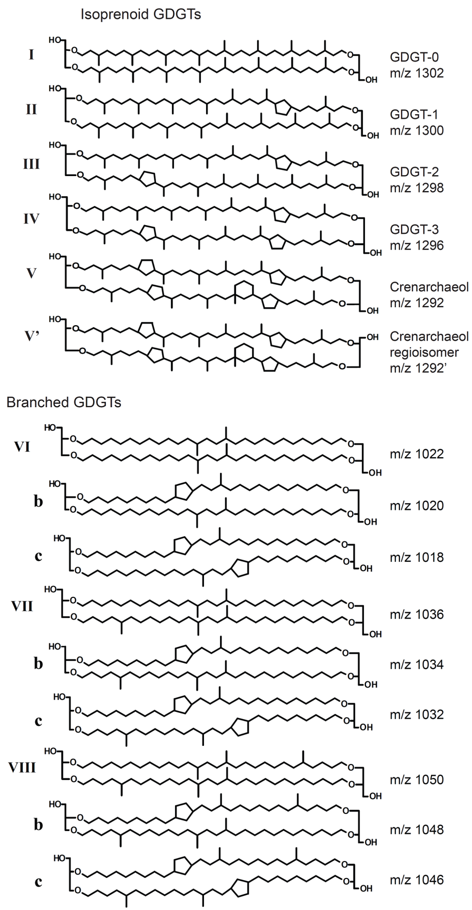

Figure A1. Key to GDGT structures.

CPD
11, 1177–1218, 2015

Short-term variability in the sedimentary BIT index of Lake Challa

L. K. Buckles et al.